Article

Stabilization of β-Hairpin Peptides by Salt Bridges: Role of Preorganization in the Energetic Contribution of Weak Interactions

Barbara Ciani, Muriel Jourdan, and Mark S. Searle

J. Am. Chem. Soc., **2003**, 125 (30), 9038-9047• DOI: 10.1021/ja030074l • Publication Date (Web): 04 July 2003

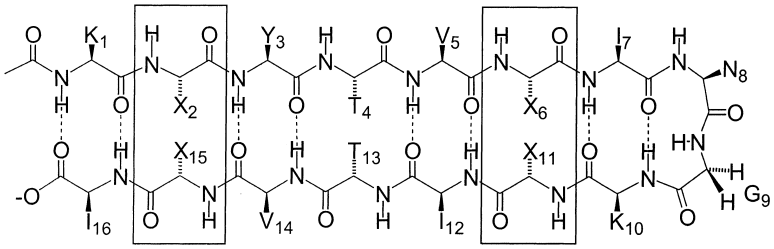

β**1**: K_2-S_{15}, S_6-K_{11} β**3**: K_2-S_{15}, E_6-K_{11}

β**2**: K_2-E_{15}, S_6-K_{11} β**4**: K_2-E_{15}, E_6-K_{11}

More About This Article

Additional resources and features associated with this article are available within the HTML version:

- Supporting Information
- Links to the 11 articles that cite this article, as of the time of this article download
- Access to high resolution figures
- Links to articles and content related to this article
- Copyright permission to reproduce figures and/or text from this article

View the Full Text HTML

J|A|C|S
ARTICLES
Published on Web 07/04/2003

Stabilization of β-Hairpin Peptides by Salt Bridges: Role of Preorganization in the Energetic Contribution of Weak Interactions

Barbara Ciani, Muriel Jourdan,† and Mark S. Searle*

Contribution from the School of Chemistry, University of Nottingham, University Park, Nottingham, NG7 2RD, U.K.

Received February 3, 2003; E-mail: mark.searle@nottingham.ac.uk

Abstract: A model β-hairpin peptide has been used to investigate the context-dependent contribution of cross-strand Lys−Glu interactions to hairpin stability. We have mutated two Ser−Lys interstrand pairs to Glu−Lys salt bridges, one close to the type I′ Asn−Gly turn sequence (Ser6 → Glu), and one close to the N- and C-termini (Ser15 → Glu). Each individual interaction contributes ∼1.2−1.3 kJ mol^{-1} to stability; however, introducing the two salt bridges simultaneously produces a much larger overall contribution (−3.6 kJ mol^{-1}) consistent with an important role for preorganization and cooperativity in determining the energetics of weak interactions. We compare and contrast CD and NMR data on the highly folded hairpin with the two Glu−Lys pairs to shed light on the nature of the folded state in water. We show that large cosolvent-induced changes in the CD spectrum, in contrast with the modest effects observed on Hα chemical shifts, support a hydrophobically collapsed entropy-driven conformation in water whose stability is modulated by long-range Coulombic interactions from the Glu−Lys interactions. Cosolvent stabilizes the structure enthalpically, as is evident from CD melting profiles.

Introduction

Hierarchical models for protein folding point to local interactions playing an important role in restricting the conformational space of the polypeptide chain in the search for the native state.[1] Autonomously folding β-hairpins, two β-strands linked by a β-turn, have emerged recently as vehicles for probing local interactions in β-sheet folding and assembly,[2] and as building blocks in protein design.[3] These data complement a large body of work on the structure and stability of isolated α-helices, and the rational design of α-helical proteins.[4] β-Hairpins have been employed for probing many aspects of conformational stability, the nature of noncovalent weak interactions, and the intrinsic conformational preferences that underlie protein folding, stability, and recognition.[5−9] Several novel motifs have recently emerged as strong structure-stabilizing interactions,[10] while phage display and combinatorial approaches have become tools in the search for structured β-sheet peptides or for novel ligands aimed at protein targets.[11] In other cases, β-sheet based motifs are emerging as possible new peptide-based drugs with constrained structures carrying bioactive motifs for highly specific recognition.[12]

It is generally regarded that salt bridges make an important contribution to the stability of the native state of proteins, this contribution is highly context-dependent, modulated by solvent

† Current address: University of Grenoble, LEDSS V, 301 rue de la Chimie BP 53, 38041 Grenoble, Cedex 9, France.

(1) (a) Honig, B. *J. Mol. Biol.* **1999**, *293*, 283−293. (b) Brockwell, D. J.; Smith, D. A.; Radford, S. E. *Curr. Opin. Struct. Biol.* **2000**, *10*, 16−25. (c) Baldwin, R. L.; Rose, G. *Trends Biochem. Sci.* **1999**, *24*, 26−33. (d) Baldwin, R. L.; Rose, G. *Trends Biochem. Sci.* **1999**, *24*, 77−83.
(2) (a) Gellman, S. H. *Curr. Opin. Chem. Biol.* **1998**, *2*, 717−725. (b) Ramirez-Alvarado, M.; Kortemme, T.; Blanco, F. J.; Serrano, L. *Bioorg. Med. Chem.* **1999**, *7*, 93−103. (c) Searle, M. S. *J. Chem. Soc., Perkin Trans. 2* **2001**, 1011−1020.
(3) (a) Ottesen, J. J.; Imperiali, B. *Nat. Struct. Biol.* **2001**, *8*, 535−539. (b) Struthers, M. D.; Cheng, R. P.; Imperiali, B. *Science* **1996**, *271*, 342−345.
(4) (a) Chakrabartty, A.; Baldwin, R. L. *Adv. Protein Chem.* **1995**, *46*, 141−176. (b) Munoz, V.; Serrano, L. *J. Mol. Biol.* **1995**, *245*, 3, 275−296. (c) O'Neil, K. T.; DeGrado, W. F. *Science* **1990**, *250*, 4981, 646−651. (d) Hill, R.; DeGrado, W. *J. Am. Chem. Soc.* **1998**, *120*, 6, 1138−1145. (e) Munoz, V.; Cronet, P.; Lopez-Hernandez, E.; Serrano, L. *Folding Des.* **1996**, *1*, 3, 167−178. (f) Viguera, A.; Villegas, V.; Aviles, F.; Serrano, L. *Folding Des.* **1997**, *2*, 1, 23−33. (g) Dalal, S.; Balasubramanian, S.; Regan, L. *Nat. Struct. Biol.* **1997**, *4*, 7, 548−552.
(5) Espinosa, J. F.; Munoz, V.; Gellman, S. H. *J. Mol. Biol.* **2001**, *306*, 397−402.
(6) Hydrophobic contacts: (a) Blanco, F. J.; Jimenez, M. A.; Herranz, J.; Rico, M.; Santoro, J.; Nieto, J. L. *J. Am. Chem. Soc.* **1993**, *115*, 13, 5887−5888. (b) DeAlba, E.; Jimenez, M. A.; Rico, M.; Nieto, J. L. *Folding Des.* **1996**, *1*, 2, 133−144. (c) Ramirez-Alvarado, M.; Blanco, F. J.; Serrano, L. *Nat. Struct. Biol.* **1996**, *3*, 604−612. (d) Searle, M. S.; Williams, D. H.; Packman, L. C. *Nat. Struct. Biol.* **1995**, *2*, 999−1006. (e) Jourdan, M.; Griffiths-Jones, S. R.; Searle, M. S. *Eur. J. Biochem.* **2001**, *267*, 3539−3548. (f) Tatko, C. D.; Waters, M. L. *J. Am. Chem. Soc.* **2002**, *124*, 9372−9373. (g) Cochran, A. G.; Skelton, N. J.; Starovasnik, M. A. *Proc. Natl. Acad. Sci. U.S.A.* **2001**, *98*, 5578−5583.
(7) (a) Maynard, A. J.; Sharman, G. J.; Searle, M. S. *J. Am. Chem. Soc.* **1998**, *120*, 1996−2007. (b) Griffiths-Jones, S. R.; Maynard, A. J.; Sharman, G. J.; Searle, M. S. *J. Mol. Biol.* **1998**, *284*, 5, 1597−1609. (c) Griffiths-Jones, S. R.; Maynard, A. J.; Searle, M. S. *J. Mol. Biol.* **1999**, *292*, 1051.
(8) Espinosa, J. F.; Gellman, S. H. *Angew. Chem.* **2000**, *39*, 2330−2333.
(9) β-turn residues: (a) Dyson, H. J.; Rance, M.; Houghten, R. A.; Lerner, R. A. *J. Mol. Biol.* **1988**, *201*, 161−200. (b) Yao, J.; Dyson, H. J.; Wright, P. E. *J. Mol. Biol.* **1994**, *243*, 736−753. (c) Yao, J.; Feher, V. A.; Espejo, B. F.; Reymond, M. T.; Wright, P. E.; Dyson, H. J. *J. Mol. Biol.* **1994**, *243*, 754−766. (d) DeAlba, E.; Jimenez, M. A.; Rico, M. *J. Am. Chem. Soc.* **1997**, *119*, 1, 175−183. (e) Haque, T. S.; Gellman, S. H. *J. Am. Chem. Soc.* **1997**, *119*, 2303−2304. (f) Ramirez-Alvarado, M.; Blanco, F. J.; Niemann, H.; Serrano, L. *J. Mol. Biol.* **1997**, *273*, 898−912. (g) Stanger, H. E.; Gellman, S. H. *Protein Sci.* **1998**, *120*, 17, 4236−4237.
(10) (a) Cochran, A. G.; Tong, R. T.; Starovasnik, M. A.; Park, E. J.; McDowell, R. S.; Theaker, J. E.; Skelton, N. J. *J. Am. Chem. Soc.* **2001**, *123*, 625−632. (b) Pastor, M. T.; Lopez de la Paz, M.; Lacroix, E.; Serrano, L.; Perez-Paya, E. *Proc. Natl. Acad. Sci. U.S.A.* **2002**, *99*, 614−619.
(11) Blandl, T.; Cochran, A. G.; Skelton, N. J. *Protein Sci.* **2003**, *12*, 237−247.

10.1021/ja030074l CCC: $25.00

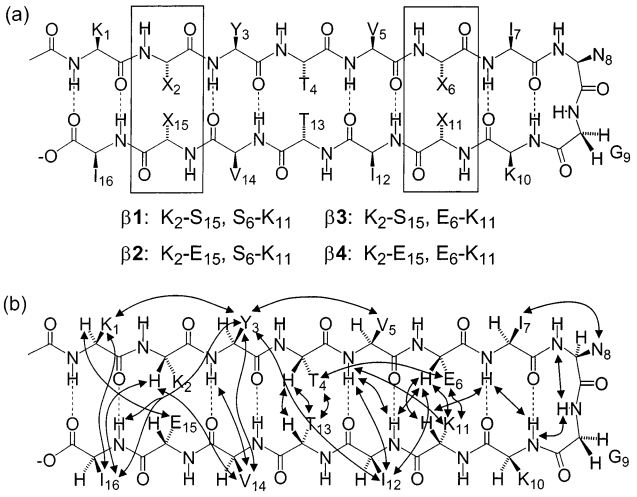

Figure 1. (a) Schematic representation of the family of β-hairpin peptides (β**1**−β**4**), showing the main chain alignment, cross-strand residue pairing, and putative hydrogen bonds. The sites of the mutated residues are indicated by "X" with boxes representing the positions of the salt bridges. (b) Structure of hairpin β**4** summarizing medium- and long-range NOEs used in the structure calculations.

accessibility and conformational constraints on the protein surface. Although some mutational analyses have shown that the energetic contribution can be vanishingly small, in other cases, involving interaction between partially buried charges, the effects can be significant.[13,14] The high abundance of ionic interactions on the surface of hyperthermophilic proteins,[15] together with examples of the rational enhancement of protein stability through the redesign of surface charge distribution, including the elimination of potentially repulsive interactions,[16] unambiguously establishes their important role in engineering protein thermostability. However, in model peptides that fold only weakly in water, the relative importance of ionic versus hydrophobic interactions in stabilizing local secondary structure has been less well studied, with reports of small free energy contributions from polar interactions commensurate with a dynamic conformation and side chains that are highly solvent exposed.[17]

We have employed a model system (peptide β**1**; Figure 1) for investigating the thermodynamics of β-hairpin folding[7] and have examined in detail the context-dependent contribution of salt bridges to hairpin folding. We have mutated two Ser−Lys interstrand pairs in β**1** to Glu−Lys salt bridges, one close to the N- and C-termini (Ser15 → Glu; peptide β**2**), and one close to the type I′ Asn-Gly turn sequence (Ser6 → Glu; peptide β**3**), and have investigated the context and pH-dependent contribution of the fully charged K^+E^- and partially charged K^+E° interactions to hairpin stability (Figure 1). We also examine the energetic effects of introducing the two salt bridges simultaneously at these two positions (peptide β**4**) and demonstrate that the net contribution is greater than the sum of the individual contributions, consistent with an important role for preorganization and cooperativity in determining the energetics of weak interactions. We compare and contrast CD and NMR data on the highly folded peptide β**4** to shed light on the nature of the folded state in water.

Materials and Methods

Peptide Synthesis and NMR Methods. All peptides were synthesized using standard solid-phase methods and purified by reverse-phase HPLC.[7] NMR data were collected on DRX500 and Avance600 Bruker spectrometers equipped with inverse-detection probes and z-field gradients for solvent-suppression using protocols and 2D NMR methodologies previously described.[7]

Peptide Aggregation. Sample aggregation was assessed by extensive dilution studies. Because a number of chemical shifts deviate significantly from random coil values, these were monitored in the range from 1.0 to 0.01 mM, as previously described.[5a] Downfield Hα shifts, arising from the folded conformation of the peptide, were unaffected by changes in peptide concentration in this range. Line widths also appeared to be concentration-independent, indicating that the peptides are essentially monomeric over this concentration range.

Structure Calculations. Starting structures were calculated using DYANA (version 1.2).[18] A total of 173 upper-limit distance restraints were derived from NOE data and classified as strong (<2.7 Å), medium (<3.8 Å), and weak (<5.0 Å); a further 24 torsion angle restraints derived from $^3J_{NH-H\alpha}$ values were also used. Thirty randomly generated structures were annealed using 4000 dynamics steps followed by 1000 minimization steps. Three of the 30 structures were randomly chosen as starting structures for simulated annealing by molecular dynamics using AMBER 6,[19] employing a total simulation time of 100 ps.[7] The SHAKE algorithm allowed a step size of 2 fs to be used, while an implicit solvent model was employed with a distance-dependent dielectric and an electrostatic cutoff of 9 Å. The last five coordinate sets collected over the last 5 ps of MD simulation were averaged to generate a single structure. Two different random seeds were employed for each of the three different starting structures, with initial velocities assigned from a Maxwellian distribution at 50 K. This approach yielded a total of six restrained structures that were subsequently averaged and energy minimized to generate the mean structure at 0 K. The N- and C-terminal residues of the six structures show the greatest flexibility; structure statistics are presented in Table 1. Unrestrained dynamics simulations on β**4** at 300 K were performed using an explicit solvent model within AMBER 6 with the peptide placed at the center of a rectangular box (47 × 35 × 41 Å^3) containing 1539 TIP3 water molecules and counterions to maintain overall charge neutrality. The SHAKE algorithm and particle mesh Ewald methods were implemented,

(12) (a) Robinson, J. A. *Synlett* **2000**, 429−441. (b) Descours, A.; Moehle, K.; Renard, A.; Robinson, J. A. *ChemBioChem* **2002**, *3*, 318−323. (c) Korsinczky, M. L. J.; Schirra, H. J.; Rosengren, K. J.; West, J.; Condie, B. A.; Anderson, M. A.; Craik, D. J. *J. Mol. Biol.* **2001**, *311*, 579−591.
(13) (a) Horovitz, A.; Serrano, L.; Avron, B.; Bycroft, M.; Fersht, A. R. *J. Mol. Biol.* **1990**, *216*, 1031−1044. (b) Strop, P.; Mayo, S. L. *Biochemistry* **2000**, *39*, 1251−1255. (c) Anderson, D. E.; Becktel, W. J.; Dahlquist, F. W. *Biochemistry* **1990**, *29*, 2403−2408. (d) Gans, P. J.; Lyu, P. C.; Manning, M. C.; Woody, R. W.; Kallenbach, N. R. *Biopolymers* **1991**, *31*, 1605−1614. (e) Scholtz, J. M.; Qian, H.; Robbins, V. H.; Baldwin, R. L. *Biochemistry* **1993**, *32*, 9668−9676.
(14) (a) Perl, D.; Mueller, U.; Heinemann, U.; Schmid, F. X. *Nat. Struct. Biol.* **2000**, *7*, 380−383. (b) Pace, C. N. *Nat. Struct. Biol.* **2000**, *7*, 345−346.
(15) (a) Karshikoff, A.; Ladenstein, R. *Trends Biochem. Sci.* **2001**, *26*, 550−556. (b) Kumar, S.; Nussinov, R. *Cell. Mol. Life Sci.* **2001**, *58*, 1216−1233. (c) Vetriani, C.; Maeder, D. L.; Tolliday, N.; Yip, K. S.; Stillman, T. J.; Britton, K. L.; Rice, D. W.; Klump, H. H.; Robb, F. T. *Proc. Natl. Acad. Sci. U.S.A.* **1998**, *95*, 12300−12305. (d) Elcock, A. H. *J. Mol. Biol.* **1998**, *284*, 489−502.
(16) (a) Takano, K.; Tsuchimori, K.; Yamagata, Y.; Yutani, K. *Biochemistry* **2000**, *39*, 12375−12381. (b) Loladze, V. V.; Ibarra-Molero, B.; Sanchez-Ruiz, J.; Makhatadze, G. I. *Biochemistry* **1999**, *38*, 16419−16423. (c) Ibarra-Molero, B.; Laladze, V. V.; Makhatadze, G. I.; Sanchez-Ruix, J. M. *Biochemistry* **1999**, *38*, 8138−8149.
(17) (a) De Alba, E.; Blanco, F. J.; Jimenez, M. A.; Rico, M.; Nieto, J. L. *Eur. J. Biochem.* **1995**, *233*, 283−292. (b) Searle, M. S.; Griffiths-Jones, S. R.; Skinner-Smith, H. *J. Am. Chem. Soc.* **1999**, *121*, 11615−11620. (c) Ramirez-Alvarado, M.; Blanco, F. J.; Serrano, L. *Protein Sci.* **2001**, *10*, 1381−1392.
(18) Güntert, P.; Mumenthaler, C.; Wüthrich, K. *J. Mol. Biol.* **1997**, *273*, 1, 283−298.
(19) (a) Pearlman, D. A.; Case, D. A.; Caldwell, J. W.; Ross, W. S.; Cheatham, T. E.; Ferguson, D. M.; Seibel, J. L.; Singh, U. C.; Weiner, P. K.; Kollman, P. A. AMBER; University of California, San Francisco, CA, 1995. (b) Pearlman, D. A.; Case, D. A.; Caldwell, J. W.; Ross, W. S.; Cheatham, T. E.; Debolt, S.; Ferguson, D. M.; Seibel, R.; Kollman, P. A. *Comput. Phys. Commun.* **1995**, *91*, 1−41.

Table 1. Structure Statistics for the Final Six NMR Structures of Hairpin β4 Calculated from Data in Aqueous Solution, 298 K

Number of Restraints	
intraresidue NOEs	93
sequential NOEs	44
medium- and long-range NOEs	36
total	**173**
dihedral angle restraints	24
Structure Statistics	
number of NOE violations > 0.2 Å	0
number of dihedral angle violations > 5°	0
ϕ/ψ distribution (%) (PROCHECK)	
favored	46.2
allowed	53.8
generous and disallowed	0
RMSD from mean structure	
backbone heavy atoms (residues 3−14)	1.05
all heavy atoms (residues 3−14)	1.60

and the pressure and temperature of the system were controlled using Berendsen's method.[20] Calculations were run over a period of 3.5 ns using a time step of 2 fs following a careful equilibration protocol over the first 10 ps in which the solvent and solute were first energy minimized. The charge state of the Glu side chains was adjusted by protonation to simulate conditions at low pH. The potential contribution of electrostatic interactions to the stability of β**4** was monitored from the time-averaged separation of the side-chain termini of the K_2-E_{15} pair and the E_6-K_{11} pair, the data were analyzed using the CARNAL module of AMBER, and the structures were displayed using MOLMOL.[21]

Circular Dichroism Spectroscopy. Circular dichroism (CD) data were collected on an Applied Photophysics π*-180 system fitted with a NESLAB circulating temperature regulator. Stock solutions of peptides were prepared as 1 mg in 1 mL of solution. Samples were diluted with water, or aqueous methanol, to give 50 μM solutions for analysis by CD. Typically, 10 scans were acquired over the wavelength range 190−250 nm in 1.0 nm steps using a bandwidth of 4 nm at 298 K and a 0.2 cm path length cell. The resulting data were averaged, smoothed, and baseline corrected by solvent subtraction. CD melting curves were obtained using a Peltier programmable heating block employing a heating rate of 1 deg min^{-1}. CD data were collected at 278 K before and after the temperature ramp. In all cases, the ellipticity over a range of wavelengths deviated by <10%, demonstrating reversibility of the melting transition.

Quantitative Analysis of Hairpin Folding. The equilibrium constant (K) for folding has been estimated assuming a two-state model in which the folded and unfolded states are in rapid equilibrium producing time-averaged chemical shifts. The justification of this model is discussed below and has been presented elsewhere.[7] More recent temperature-jump studies,[22] including kinetic experiments using our original model system β**1**,[23] have confirmed that folding can be adequately described by a single activation barrier separating the folded and unfolded states, consistent with a two-state model. We have used an RMS deviation in Hα chemical shifts from random coil values (taken over all residues) as a measure of the extent to which a given hairpin is folded at 298 K, given that all residues appear to be perturbed in a similar manner.[7] An estimate of the concentration of the folded state can be deduced from the experimentally determined RMS$\Delta\delta_{H\alpha}$ provided limiting values for the fully folded and fully unfolded states are known. While the latter is taken as zero, in agreement with experimental data from other hairpin analogues which show little evidence for folding, the limiting value for the folded state is subject to greater uncertainty. Data for β**4** in 50% methanol at 278 K were used as a reasonable estimate for the fully folded state (RMS$\Delta\delta_{H\alpha}^{limit}$).

Thus,

$$K_{eq} = [\text{folded}]/[\text{unfolded}]$$

where

$$K_{eq} = 1/[1 - (\text{RMS}\Delta\delta_{H\alpha}/\text{RMS}\Delta\delta_{H\alpha}^{\ limit})]$$

and

$$\Delta G = -\text{RT}\ln(K_{eq}) \quad (1)$$

Errors in $\Delta\Delta G$ values, corresponding to differences in stability between hairpins, are estimated to be ca. ±0.3 kJ mol^{-1}, reflecting propagation errors from experimental uncertainties in $\delta_{H\alpha}$ values of approximately ±0.01 ppm.

CD melting curves were recorded at 217 nm, and the temperature-dependence of the mean residue ellipticity was fit to the following expressions where the equilibrium constant K_{eq} is defined in terms of the observed ellipticity, θ_{obs}, and the limiting values for the folded and unfolded states, θ_F and θ_U, respectively, by $K_{eq} = (\theta_{obs} - \theta_U)/(\theta_F - \theta_{obs})$. When one assumes that the temperature-dependence of ΔG follows the standard thermodynamic relationships, then the dependence of θ_{obs} on T is given by the equation:

$$\theta_{obs} = \{\theta_F \exp[-x] + \theta_U\}/\{1 + \theta_F \exp[-x]\} \quad (2)$$

where

$$x = 1/RT[\Delta H + \Delta C_p(T - 298) - T(\Delta S + \Delta C_p \ln(T/298))]$$

Fitting the experimental value for θ_{obs} to eq 1 has enabled ΔH, ΔS, and ΔC_p for folding to be determined in water and various aqueous methanol mixtures. θ_F, the limiting value for the fully folded state, was taken as −11 600 deg cm^2 mol^{-1} from the data for β**4** in 50% methanol at 278 K where the sigmoidal part of the folding curve is most clearly evident. This value is close to that predicted for a β-sheet with this number of residues, which justifies our assumption that the peptide is close to being fully folded under these conditions. θ_U, the limiting value for the unfolded state, was taken as −600 deg cm^2 mol^{-1} from data for an isomeric peptide of identical composition but different sequence that shows no evidence for folding by CD or NMR.

Results and Discussion

Hairpin Conformation in Solution by NMR. All four β-hairpin peptides have been analyzed in detail by NMR and show the expected pattern of NOEs consistent with the alignment of β-strands shown in Figure 1a. A selection of medium- and long-range NOEs observed for hairpin β**4** in aqueous solution at pH 5.5 are shown in Figure 1b. The effect of the introduction of salt bridges at various positions on the relative populations of the folded state is most readily illustrated by examining the deviation of Hα chemical shifts from random coil values[24] ($\Delta\delta_{H\alpha}$ values) at pH 5.5; the pattern of $\Delta\delta_{H\alpha}$ values is consistent with a β-hairpin structure with two extended β-strand regions (+$\Delta\delta_{H\alpha}$ values) separated by a β-turn (−$\Delta\delta_{H\alpha}$ values).[25,26] The data in Figure 2 establish unambiguously that

(20) (a) York, D. M.; Darden, T. A.; Pedersen, L. G. *J. Chem. Phys.* **1993**, *99*, 8345−8348. (b) Jorgensen, W. L.; Chandrasekhar, J.; Madura, J. D.; Impey, R. W.; Klein, M. L. *J. Chem. Phys.* **1983**, *79*, 926−935.
(21) Koradi, R.; Billeter, M.; Wuthrich, K. *J. Mol. Graphics* **1996**, *14*, 51.
(22) Munoz, V.; Thompson, P. A.; Hofrichter, J.; Eaton, W. A. *Nature* **1997**, *390*, 196.
(23) (a) Andersen, N. H.; Dyer, R. B.; Fesinmeyer, R. M.; Gai, F.; Liu, Z.; Neidigh, J. W.; Tong, H. *J. Am. Chem. Soc.* **1999**, *121*, 9879−9880. (b) Andersen, N. H.; Dyer, R. B.; Fesinmeyer, R. M.; Gai, F.; Maness, S.; Werner, J. H. *Peptides 2000: Proc. 26th Eur. Peptide Symp.*; Martinez, J., Fehrentz, J.-A., Eds.; EDK, Paris, France, 2001; pp 553−554.

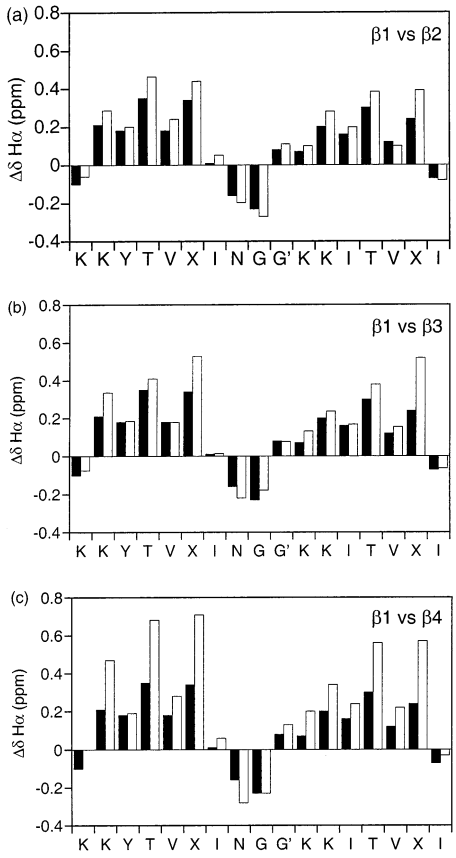

Figure 2. Changes in Hα chemical shifts ($\Delta\delta_{H\alpha}$ values) for the various mutations as compared to the reference state β**1** containing Lys−Ser cross-strand pairs at the two sites. (a) β**1** versus β**2**; (b) β**1** versus β**3**; and (c) β**1** versus β**4**. All data are at 298 K and pH 5.5.

the selective introduction of an ion pairing interaction at either position enhances the stability of the folded state by increasing the magnitude of $\Delta\delta_{H\alpha}$ values; this effect is particularly pronounced for the doubly mutated hairpin β**4** (Figure 2c) where salt bridges are simultaneously introduced adjacent to the turn sequence (E_6-K_{11}) and close to the N- and C-termini (K_2-E_{15}). The smaller population of the folded state evident for β**2** and β**3** from the chemical shift analysis is also reflected in fewer NOEs, although the interactions observed are entirely consistent with all hairpins folding in an analogous manner.

We have determined a detailed solution structure of β**4** on the basis of extensive interstrand NOE data in aqueous solution that arises from the high population of the folded state and the excellent chemical shift dispersion in the NH and Hα region of the spectrum (Figure 3). The main chain alignment and putative hydrogen-bonding pattern are confirmed by a number of interstrand Hα ↔ Hα, Hα ↔ NH, and NH ↔ NH NOEs. In general, $NH_i \leftrightarrow NH_{i+1}$ sequential NOEs are very weak or absent, while $H\alpha_i \leftrightarrow NH_{i+1}$ NOEs are very strong, consistent with extended β-strand conformation for residues 1−7 and 10−16. The strong $NH_i \leftrightarrow NH_{i+1}$ NOE between G_9 and K_{10} is consistent

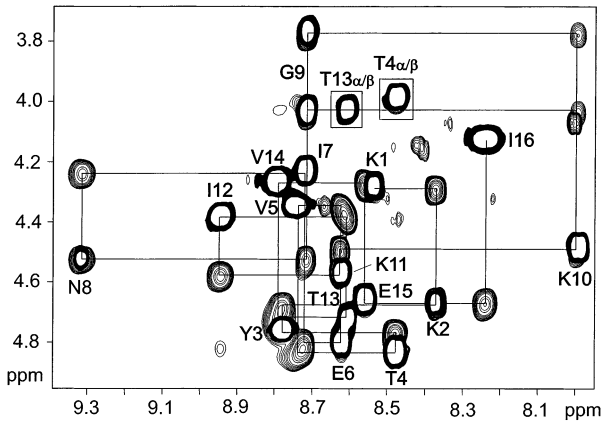

Figure 3. Overlayed fingerprint regions of 2D TOCSY and NOESY data (200 ms) of β**4** (298 K, aqueous solution at pH 5.5), showing NH and Hα chemical shift dispersion and NH−Hα connectivities used in the sequential assignment of the peptide backbone; unfilled TOCSY cross-peaks (darker contours) are indicated with residue assignments.

with a sharp change in backbone direction indicative of a β-turn. This is also clearly apparent from the relative intensity of sequential versus intraresidue $NH_i-H\alpha_{i+1}$ and $NH_i-H\alpha_i$ backbone NOE intensities.[7,26,27] In extended β-strands, the former is significantly more intense than the latter (ratio > 5); however, at the I_7-N_8 step, this intensity ratio lies close to unity (see Figure 3), which, together with a small $^3J_{NH-H\alpha}$ value for N_8 < 5 Hz, is a clear indication of the change in direction of the main chain associated with a type I′ reverse turn conformation. The excellent chemical shift dispersion has enabled NOEs from the side chains of K_2, E_6, K_{11}, and E_{15} to be identified that demonstrate that the aliphatic portions of these residues form hydrophobic contacts with adjacent residues (T_4 and T_{13}) as well as interactions between strands. Although we cannot identify directly salt bridges between these pairs of residues, the side-chain orientations on the face of the hairpin are consistent with these interactions. In addition, the side chain of Y_3 shows many potentially stabilizing hydrophobic contacts to adjacent Val and Ile residues, confirming that these residues are located on the same face of the β-hairpin. Using torsion angle driven dynamics (DYANA v3.0),[18] and restrained molecular dynamics (MD) simulations (AMBER 6),[19] we have generated a family of NMR structures and an average structure (Figure 4; see Table 1) that demonstrate the right-handed twist typical of a protein β-sheet facilitated by a type I′ NG turn. The backbone conformation is generally well defined by the restraints; however, the N- and C-terminal residues K_1 and I_{16} show greater flexibility with some structures, suggesting that K_1, which is relatively unrestrained by adjacent residues, is able to fold back and form electrostatic interactions with E_{15}. Thus, electrostatic contributions from the interaction of E_{15} with both K_1 and K_2 are likely to contribute to hairpin stability.

Molecular Dynamics Simulations Probe Time-Averaged Electrostatic Interactions. Although the structure calculations described above define the peptide backbone conformation with some precision, few experimental restraints define the orientation of the flexible side chains of Glu and Lys residues or whether there is any persistent electrostatic interaction between them.

(24) Wuthrich, K. *NMR of proteins and nucleic acids*; John Wiley & Sons: New York, 1986.
(25) (a) Wishart, D. S.; Sykes, B. D.; Richards, F. M. *J. Mol. Biol.* **1991**, *222*, 311. (b) Wishart, D. S.; Sykes, B. D.; Richards, F. M. *Biochemistry* **1992**, *31*, 1647.
(26) Sharman, G. J.; Griffiths-Jones, S. R.; Jourdan, M.; Searle, M. S. *J. Am. Chem. Soc.* **2001**, *123*, 12318−12324.
(27) (a) Fiebig, K. M.; Schwalbe, H.; Buck, M.; Smith, L. J.; Dobson, C. M. *J. Phys. Chem.* **1996**, *100*, 2661−2666. (b) Serrano, L. *J. Mol. Biol.* **1995**, *254*, 322−333. (c) Smith, L. J.; Bolin, K. A.; Schwalbe, H.; Macarthur, M. W.; Thornton, J. M.; Dobson, C. M. *J. Mol. Biol.* **1996**, *255*, 494−506.

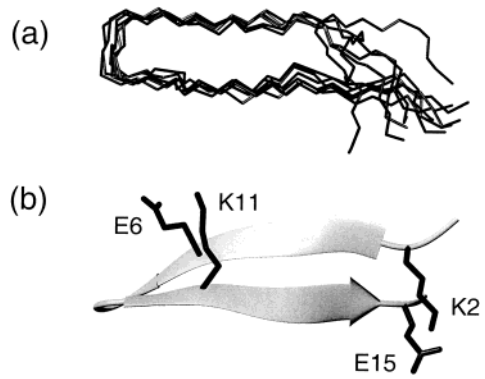

Figure 4. (a) Overlay of six NOE-restrained NMR structures of β**4** calculated from data in aqueous solution showing the backbone fold and twisted antiparallel β-strand conformation; (b) ribbon representation of the averaged energy-minimized structure of β**4** showing the position and orientation of the Lys−Glu salt bridges.

Previous studies have used molecular dynamics simulations to probe a range of contributions to the folding of model β-hairpin and antiparallel β-sheets, including the influence of β-turn residues, salt bridges, and more fundamental aspects of the mechanism of folding.[7,28] The time-averaged proximity of the charged side-chain pairs of K_2-E_{15} and E_6-K_{11} was examined during 3.5 ns of unrestrained MD simulation at 300 K using an explicit solvent model. To simulate low pH conditions, the charges on the Glu side chains were neutralized, and the 3.5 ns dynamics calculations were repeated. Under these conditions, the hairpin shows little tendency to unfold with the register of cross-strand hydrogen-bonding interactions stable throughout the simulations. The random fluctuation in side-chain dynamics during the course of the two trajectories is shown in Figure 5A−D. The distance (Å) between the Lys Nϵ and Glu Cδ is plotted against time for the two pairs of interactions involving a fully charged Glu side chain (A and B) and a protonated Glu side chain (C and D). The charge state of the Glu side chains appears to have a significant effect on the average proximity of the two side chains and their flexibility. As is evident in Figure 5A and B, the side chains fluctuate between the ideal geometry for a salt bridge (N$\epsilon-$Cδ < 4 Å) and extended conformations (N$\epsilon-$Cδ > 6 Å) in which the two are solvent exposed. The average distances throughout the simulation (4.8 ± 1.3 and 5.3 ± 1.5 Å for K_2-E_{15} and E_6-K_{11}, respectively, including one standard deviation) are similar, suggesting only a small context-dependence. Both pairs of charged residues form persistent short-range interactions (N$\epsilon-$Cδ < 4 Å), consistent with stable salt bridges for up to ~500 ps at a time before breaking and adopting solvent exposed conformations, only to reform subsequently. The N$\epsilon-$Cδ separation considered indicative of a salt bridge lies between 3.5 and 4.5 Å. Using the upper limiting value, the two interactions (E_6-K_{11} and K_2-E_{15}) persist for 64% and 75% of the simulation, respectively. Neutralization of the Glu side chain by protonation results in greater side-chain dynamics, diminishing the population of close-range interactions for $K_{11}-E_6^{COOH}$ and $K_2-E_{15}^{COOH}$ to 18% and 10%, respectively (Figure 5C and D). The average N$\epsilon-$Cδ distance throughout the 3.5 ns simulation increases to 5.9 ± 1.5 and 6.6 ± 1.8 Å, respectively, indicating that solvent is much more competitive at binding to the polar headgroups and disrupting the interaction when the side chains are only partially charged. Thus, our structural model, derived from experimental restraints, coupled with MD simulations, is consistent with time-averaged stabilizing contributions from salt bridges on the polar face of the hairpin. The effect of neutralizing the charge on both Glu residues is to significantly reduce the amount of time the side chains spend in sufficiently close proximity to form a direct hydrogen bond, suggesting that a reduction in pH below the pK_a of the Glu side chains should have a net destabilizing effect on the folded conformation of the hairpin.

Cooperative Interactions in Hairpin Stabilization. A striking observation from the analysis of the chemical shift data shown in Figure 2a and b for the single mutants β**2** and β**3** is that the introduction of stabilizing interactions at specific sites produces global changes in Hα chemical shifts, consistent with a two-state folding model. For example, introducing the ionic interaction between K_2 and E_{15} produces a small increase in stability which is sensed by all residues including those in the β-turn. Similarly, introducing a salt bridge close to the turn sequence (β**3**) produces long-range stabilization along the β-hairpin such that residues close to the N- and C-termini also reflect an increase in the population of the folded state. A recent study of a family of isomeric 20-mers has focused on the effects on stability of a localized stabilizing aromatic cluster as a function of its separation from the turn sequence.[6] While a small separation between turn and hydrophobic cluster leads to greater stability of a subset of core interactions, fewer residues are found to be involved in cross-strand interactions between β-strands, and a greater proportion of residues are disordered at the N- and C-termini. These data contrast with our results for the β**1** family of peptides where end-fraying effects are confined to the two terminal residues, and the interactions that contribute to hairpin stability are widely distributed along the sequence. The two systems reflect the sequence-dependent manner in which the peptide chain can be predisposed to fold in solution, reflecting the nature and distribution of the interresidue contacts formed.

In the current context, the energetic contribution of introducing each Glu−Lys salt bridge should depend on the extent to which the hairpin is already preorganized to facilitate this interaction. Where the entropic cost of bringing the two functional groups together is smaller, as might be the case when there is greater preorganization of the peptide backbone, then, in principle, the greater is the stabilization energy available from this interaction.[29] To test this hypothesis, we have calculated $\Delta\Delta G$ values for β**2**, β**3**, and β**4**, representing the increase in hairpin stability for the K−E mutations with respect to the K−S

(28) (a) Kamiya, N.; Higo, J.; Nakamura, H. *Protein Sci*. **2002**, *11*, 2297−2307. (b) Lee, J.; Shin, S. *J. Phys. Chem. B* **2002**, *106*, 8796−8802. (c) Jang, H.; Hall, C. K.; Zhou, Y. Q. *Biophys. J.* **2002**, *83*, 819−835. (d) Zhou, Y. Q.; Linhananta, A. *Proteins: Struct., Funct., Genet.* **2002**, *47*, 154−162. (e) Ferrara, P.; Caflisch, A. *J. Mol. Biol.* **2001**, *306*, 837−850. (f) Garcia, A. E.; Sanbonmatsu, K. Y. *Proteins* **2001**, *42*, 345−354. (g) Ma, B. Y.; Nussinov, R. *J. Mol. Biol.* **2000**, *296*, 1091−1104. (h) Bonvin, A. M. J. J.; van Gunsteren, W. F. *J. Mol. Biol.* **2000**, *296*, 255−268. (i) Pande, V. S.; Rokhsar, D. S. *Proc. Natl. Acad. Sci. U.S.A.* **1999**, *96*, 9062−9067. (j) Dinner, A. R.; Lazaridis, D.; Karplus, M. *Proc. Natl. Acad. Sci. U.S.A.* **1999**, *96*, 9068−9073. (k) Wang, H. W.; Sung, S. S. *Biopolymers* **1999**, *50*, 763−776. (l) Sheinerman, F. B.; Brooks, C. L. *J. Mol. Biol.* **1998**, *278*, 439−456. (m) Constantine, K. L.; Friedrichs, M. S.; Stouch, T. R. *Biopolymers* **1996**, *39*, 591−614. (n) Pugliese, L.; Prevost, M.; Wodak, S. J. *J. Mol. Biol.* **1995**, *251*, 432−447.

(29) (a) Williams, D. H.; Maguire, A. J.; Tsuzuki, W.; Westwell, M. S. *Science* **1998**, *280*, 711. (b) Searle, M. S.; Sharman, G. J.; Groves, P.; Benhamu, B.; Beauregard, D. A.; Westwell, M. S.; Dancer, R. J.; Maguire, A. J.; Try, A. C.; Williams, D. H. *J. Chem. Soc., Perkin Trans. 1* **1996**, 2781−2786. (c) Searle, M. S.; Westwell, M. S.; Williams, D. H. *J. Chem. Soc., Perkin Trans. 2* **1995**, 141−151.

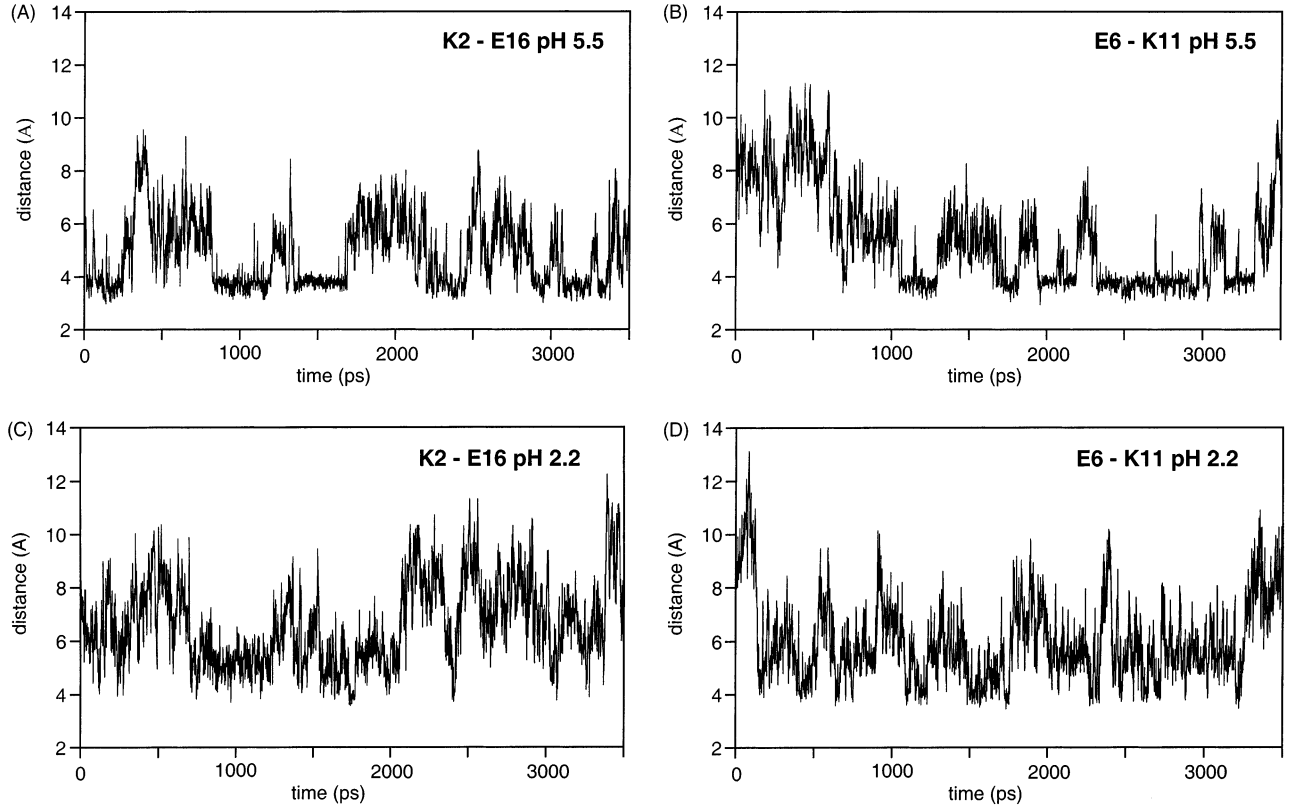

Figure 5. Time-dependent proximity (Lys Nϵ−Glu Cδ) of the charged headgroups involved in salt bridge formation during 3.5 ns of unrestrained MD simulation at 300 K in explicit solvent: (A) and (B) with E_6 and E_{15} side chains fully charged, and (C) and (D) with Glu side chains neutralized through protonation.

interactions of β**1**. Where the contributions of the two interactions are simply additive, then

$$|\Delta\Delta G^{\beta 4}| \approx |\Delta\Delta G^{\beta 2}| + |\Delta\Delta G^{\beta 3}|$$

but where the effects are cooperatively linked, then

$$|\Delta\Delta G^{\beta 4}| > |\Delta\Delta G^{\beta 2}| + |\Delta\Delta G^{\beta 3}|$$

We now examine this proposition in more detail.

Quantitative Estimates to Hairpin Stability of Charged Lys−Glu Pairs. We have assumed a simple two-state folding model to determine free energy contributions to folding.[7,30] The temperature-dependence of $\Delta\delta_{H\alpha}$ values demonstrates that all residues reflect similar changes in the proportion of the folded state, indicative of a uniform cooperative two-state unfolding process. T-jump folding/unfolding studies with hairpin peptides of similar length[22,23] have established that a single activation barrier separates the unfolded from the folded ensemble, supporting the approximation of a two-state model for folding. In the current context, the observation that all residues show a similar temperature-dependence of $\Delta\delta_{H\alpha}$ values has led us to use an RMS value for $\Delta\delta_{H\alpha}$ (RMS$\Delta\delta_{H\alpha}$) calculated over all residues as a single measure of stability under a given set of conditions. While limiting $\Delta\delta_{H\alpha}$ values for the unfolded state are well approximated by data from model peptides such as Gly−Gly−Xaa−Ala,[24] or by using β-strand sequences that do not form intermolecular interactions,[6−8,30] the best method of determining limiting $\Delta\delta_{H\alpha}$ values for the fully folded state continues to be a contentious issue because of the intrinsic problem of dealing with flexible systems. One recent approach has been to use cyclic hairpin analogues as models of the fully folded state;[8,30] alternatively, organic cosolvents promote folding and give approximate limiting values, as previously discussed.[2,7] Although changes in $\Delta\delta_{H\alpha}$ values in some cases are small (see Figure 2), chemical shifts prove to be very sensitive to small changes in stability largely because ΔG in these systems lies close to zero. In cases where the population of the folded state is already very large (>90% folded), then small additional changes in ΔG would produce only comparatively small effects on $\Delta\delta_{H\alpha}$ values.

Table 2. Hairpin Stabilities Estimated from NMR Hα Chemical Shift Data on Peptides in Aqueous Solution (298 K)[a]

	ΔG (pH 5.5)	ΔG (pH 2.2)
β1	+1.2	+2.6
β2	0	+2.3
β3	−0.1	+0.6
β4	−2.4	+0.1

[a] Errors are estimated to be less than ±0.3 kJ mol^{-1}, reflecting experimental uncertainties in $\delta_{H\alpha}$ values of approximately ±0.01 ppm, in agreement with previous estimates.[10,30]

The contribution of individual salt bridges to overall stability, measured from the relative stabilities of β**2** versus β**1** and β**3** versus β**1**, are relatively small, −1.2 and −1.3 kJ mol^{-1}, respectively (see Table 2). However, the combined effect of the two Lys−Glu salt bridges introduced simultaneously produces a significant enhancement of stability of β**4** versus β**1** of −3.6 kJ mol^{-1}. This effect is readily apparent from the

(30) (a) Syud, F. A.; Espinosa, J. F.; Gellman, S. H. *J. Am. Chem. Soc.* **1999**, *121*, 11577−11578. (b) Syud, F. A.; Stanger, H. E.; Gellman, S. H. *J. Am. Chem. Soc.* **2001**, *123*, 8667−8668.

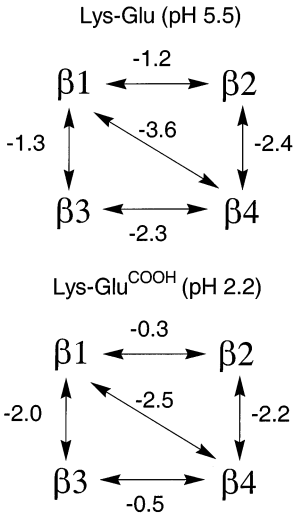

Figure 6. Thermodynamic cycles showing the context-dependent energetic contribution to hairpin stability of each electrostatic interaction by comparing relative hairpin stabilities at 298 K determined from NMR chemical shift data. (top) $\Delta\Delta G$ values for Lys−Glu interactions at pH 5.5; (bottom) $\Delta\Delta G$ values for Lys−Glu^{COOH} interactions at pH 2.2.

large increase in $\Delta\delta_{H\alpha}$ values evident in Figure 2c where the population of the folded state increases from 38% (*β***1**) to 72% (*β***4**). Thus, the contribution from a given interaction appears to be dependent on the relative stability of the system in which the interaction is being measured. Similar observations have been reported using a disulfide cyclized *β*-hairpin scaffold.[31] The indication is that the strength of the interaction appears to depend on the degree of preorganization of the *β*-hairpin template that pays varying degrees of the entropic cost in bringing the pairs of side chains together. This is more clearly illustrated by the schematic representation shown in Figure 6, which shows the thermodynamic cycle, indicating the effects on stability of the introduction of each mutation. Thus, the energetic contribution of the S_{15}/E_{15} mutation could be measured either from *β***1** ↔ *β***2** or from *β***3** ↔ *β***4**. The values obtained are quite different, the latter suggesting that the interaction is more favorable (−1.2 versus −2.3 kJ mol^{-1}). This appears to correlate with the fact that the stability of *β***3** is greater than *β***1** and that the degree of preorganization of the former determines the energetic contribution of the interaction. The same principle is evident when determining the energetics of the E_6-K_{11} interaction. This can be estimated from *β***1** ↔ *β***3** or *β***2** ↔ *β***4**. Again, the energetics are quite different (−1.3 versus −2.4 kJ mol^{-1}) with the larger contribution from the *β***2** ↔ *β***4** pair where the intrinsic stability of the *β***2** reference state is higher.

Effects of Charge Neutralization on Hairpin Stability. At pH 2.2 (below the pK_a of the carboxylate groups of the Glu side chains), all hairpins show a reduction in stability consistent with the protonation of Glu side chains reducing the Coulombic interaction between interstrand Lys−Glu ion pairs. In a previous study, we have shown that the C-terminal carboxylate group of I_{16} also contributes to the stability of *β***1** by ∼1 kJ mol^{-1} through an interaction with the side chain of K_1. At low pH, this interaction is also negated, reducing the stability of all hairpins to the same extent. Thus, quantitative estimates of relative hairpin stabilities at pH 2.2 enable us to assess the contribution of the partially charged $K^+E°$ interactions along with their context-dependence. Using a thermodynamic cycle similar to that described above (Figure 5), the $K_2{}^+-E_{15}°$ interaction can be estimated from *β***1** ↔ *β***2** and from *β***3** ↔ *β***4**; in each case, the contribution is small (−0.3 and −0.5 kJ mol^{-1}, respectively), regardless of the intrinsic stability of the hairpin. Thus, while the fully charged E_{15} has a significant effect in stabilizing the hairpin at pH 5.5 through salt bridges with K_2 and possibly K_1, when this interaction is negated at pH 2.2, *β***2** is only marginally more stable than *β***1**. Thus, in this position close to the N- and C-termini, the Coulombic interaction from K^+E^- has a net stabilizing effect when side chains are fully charged; however, the contribution from the interaction between the partially charged $K^+E°$ pairs is small, presumably because a persistent short-range hydrogen bond is required to add significantly to stability. Side-chain dynamics may preclude such a persistent interaction irrespective of the degree of preorganization of the hairpin template. This conclusion is entirely consistent with the results of our MD simulations in which neutralization of the charge of the Glu side chains results in a significant increase in the average Nϵ−Cδ distance such that a direct hydrogen bond is present for <10% of the simulation.

When we examine the contribution of the $K_{11}{}^+-E_6°$ interaction experimentally using either the *β***1** ↔ *β***3** or the *β***2** ↔ *β***4** stability difference, we observe that the energetics are similar (−2.0 and −2.2 kJ mol^{-1}) and that this interaction still contributes significantly to stability, suggesting that Glu is more stabilizing per se than Ser in this context. A number of successfully designed hairpins have polar residues in the −B2 position prior to a type I′ turn,[30] suggesting an energetically favorable interaction. Statistical analysis of interactions across antiparallel *β*-sheet shows that KE pairs are abundant in both hydrogen-bonded and non-hydrogen-bonded sites,[32] although data at low pH are generally not available to substantiate the energetic contribution when the pair of residues is only partly charged. However, data on the energetics of side-chain interactions in helices have examined pH-dependent effects on stabilities and determined the energetics for both K^+E^- (fully charged) and $K^+E°$ (partially charged) interactions.[33] When an *i*, *i* + 3 relationship is considered, the K^+E^- salt bridge can contribute ∼1.2 kJ mol^{-1}, while the $K^+E°$ interaction appears to be only marginally less stable (∼1 kJ mol^{-1}). Studies of interhelical energetic contributions to coiled-coil proteins have demonstrated greater stabilizing effects from KE pairs at low pH where the Glu side chain is protonated. The greater helical preference of E° and, in particular, the greater hydrophobicity of the side chain as compared to the fully ionized state are suggested to compensate for the absence of the Coulombic interaction at low pH.[34] These conclusions seems to be consistent with our own data for the E_6-K_{11} hairpin interaction that shows that K^+E^- and $K^+E°$, in this context at least, are both stabilizing interactions with only a small difference in energetic contribution. This seems to reflect the fact that the contribution to

(31) Russell, S. J.; Blandl, T.; Skelton, N. J.; Cochran, A. G. *J. Am. Chem. Soc.* **2003**, *125*, 388−395.

(32) (a) Hutchinson, E. G.; Sessions, R. B.; Thornton, J. M.; Woolfson, D. K. *Protein Sci.* **1998**, *7*, 1−14. (b) Cootes, A. P.; Curmi, P. M. G.; Cunningham, R.; Donnelly, C.; Torda, A. E. *Proteins: Struct., Funct., Genet.* **1998**, *32*, 175−189. (c) Merkel, J. S.; Sturtevant, J. M.; Regan, L. *Structure* **1999**, *7*, 1333−1343.

(33) Smith, J. S.; Sholtz, J. M. *Biochemistry* **1998**, *37*, 33−40.

(34) (a) Zhou, N. E.; Kay, C. M.; Hodges, R. S. *Protein Eng.* **1994**, *7*, 1365−1372. (b) Hohn, W.; Kay, C. M.; Hodges, R. S. *Protein Sci.* **1995**, *4*, 237−250. (c) Kuhlman, B.; Yang, H. Y.; Boice, J. A.; Fairman, R.; Raleigh, D. P. *J. Mol. Biol.* **1997**, *270*, 640−647.

stability from each Lys−Glu pair needs to be considered not just in terms of the electrostatic component. The preorganization of the peptide backbone in close proximity to the β-turn may facilitate stabilizing hydrophobic contacts involving the Glu side chain and other adjacent residues.[35] When the Glu side chain is fully charged, these favorable contacts may be balanced by the desolvation costs of partially burying the charge. Thus, the energetic contribution to the stability of the Lys−Glu pair needs to be considered as the sum of the various contributions from solvation effects, hydrophobicity, and electrostatic interactions between side chains. In an earlier study, we similarly concluded that the aliphatic side chain of Lys makes a significant hydrophobic contribution to the overall energetics of ion pair formation.[17b]

Studies of the energetics of salt bridges in the context of surface interactions in proteins and other model peptide systems clearly highlight a complex balance between direct charge−charge interactions, secondary effects from other polar groups, and desolvation effects, all of which are highly context-dependent.[36] Together, these factors can result in net contributions from salt bridges that are either neutral, stabilizing, or destabilizing. Neutral or destabilizing effects appear to reflect the high desolvation costs associated with placing the two charges in a low dielectric environment. Largely for this reason, experimental and theoretical studies seem to agree that salt bridge residues generally are not expected to provide as much stabilization to proteins as a pair of hydrophobic residues of similar size.[36]

We conclude that at pH 5.5 where fully charged Lys and Glu side chains can contribute significantly to hairpin stability we see that the two interactions are cooperatively linked with the enhanced stability resulting from one interaction increasing the energetic contribution of the other through preorganization of the hairpin template. However, at low pH, the interactions of uncharged E_{15} contribute little more to the stability than do those of S_{15}, presumably on the grounds that the side-chain dynamics preclude a persistent short-range hydrogen-bonding interaction or significant hydrophobic contacts regardless of the intrinsic hairpin stability. Under these conditions, the two sets of interactions are decoupled from each other, although context-dependent effects show that the E_6-K_{11} interaction contributes significantly to stability even when the Glu is protonated.

Thermal- and Solvent-Induced Changes in Hairpin Stability. A number of studies have demonstrated discrepancies between CD and NMR in estimations of the population of the folded state,[2] with hairpins that appear to be significantly folded by NMR giving rise to a largely random coil CD spectrum. One interpretation of these observations is that in aqueous solution the peptides fold as a collapsed state dominated by side-chain interactions with an ill-defined hydrogen-bonding network. In this context, Coulombic interactions between fully charged side chains lend themselves better to the stabilization of a dynamic collapsed conformation because the magnitude of the electrostatic interaction operates over a significant distance and is not orientation-dependent. There is considerable evidence that charge−charge interactions are the key adaptive mechanism underlying the enhanced stability of proteins from hyperthermophiles.[15] This adaptation has, at least in part, been attributed to the reduction in the charge desolvation penalty at higher temperatures, which enhances the electrostatic stabilization energy.

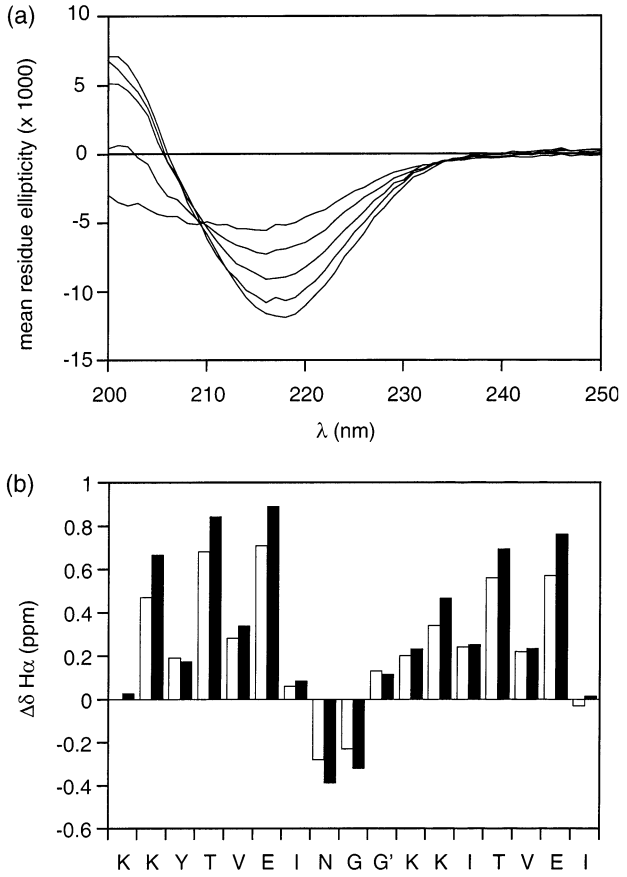

Figure 7. (a) CD spectra of β**4** showing effects of methanol concentration on the population of the folded state; ellipticity at 217 nm becomes more negative in the order 0%, 10%, 20%, 30%, and 50% v/v methanol, pH 5.5 at 298 K, [peptide] = 50 μM; (b) comparison of $\Delta\delta_{H\alpha}$ values for β**4** in water (open bars) and 50% MeOH (solid bars), pH 5.5, 298 K.

We address the issues regarding thermal- and solvent-induced changes in stability in the context of hairpin β**4**, which, as already discussed, is significantly folded as judged by a number of NMR parameters. Initially, CD data were collected at 298 K over a range of methanol concentrations between 0% and 50%. The spectrum in water alone is clearly indicative of a significant population of the folded state; however, the ellipticity at 217 nm becomes significantly more negative at higher methanol concentrations, reaching a limiting value around 50% methanol. The ellipticity at 217 nm increases by approximately 100% (see Figure 7a) over this range. In contrast, the effects on Hα chemical shifts are less pronounced, increasing by an average of 25% over the same methanol concentration range (Figure 7b). NMR chemical shifts were compared at both 1 mM and 0.01 mM peptide concentrations, with little evidence of concentration-dependent effects on the spectra. CD data were collected within the same range at a concentration of 50 μM. Thus, the large changes in the CD spectra appear to be consistent with a solvent-induced reduction in backbone flexibility con-

(35) At pH 2.2, the chemical shifts of the side-chain protons of many Glu and Lys residues are considerably overlapped precluding the unambiguous assignment of NOEs from the $C\gamma H_3$ of T4 and/or T13 to the side chain of E_6°.

(36) (a) Wimley, W. C.; Gawrisch, K.; Creamer, T. P.; White, S. H. *Proc. Natl. Acad. Sci. U.S.A.* **1996**, *93*, 2985−2990. (b) Hendsch, Z. S.; Tidor, B. *Protein Sci.* **1994**, *3*, 211−226. (c) Waldburger, C. D.; Schildbach, J. F.; Sauer, R. T. *Nat. Struct. Biol.* **1995**, *2*, 122−128. (d) Makhatadze, G. I.; Loladze, V. V.; Ermolenko, D. N.; Chen, X.; Thomas, S. T. *J. Mol. Biol.* **2003**, *327*, 1135−1148.

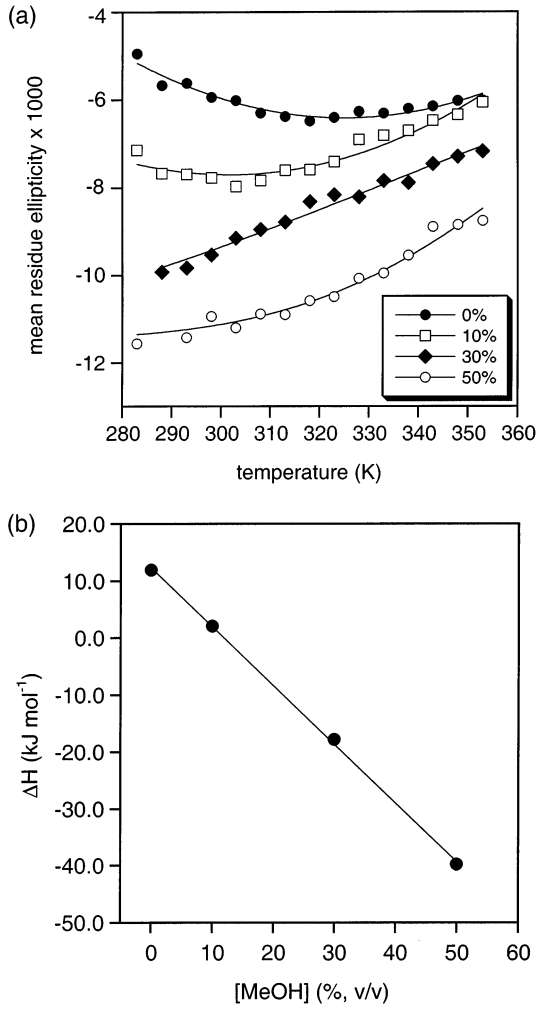

Figure 8. (a) CD melting curves for β**4** at various concentrations (% v/v) of MeOH, as indicated. The nonlinear least-squares fit to eq 2 is shown in each case. (b) Correlation between ΔH for folding and [MeOH] derived from the melting curves shown in (a). Thermodynamic parameters are given in Table 1.

sistent with a stabilization of the hydrogen-bonded structure. Studies with cyclic β-hairpin analogues seem to support this hypothesis. In these systems, the folded population is fixed (100%) by the covalent structure of the peptide; however, cosolvent-induced changes in the CD spectrum are still apparent even though the Hα shifts appear to be independent of cosolvent concentration.[2b]

The thermal unfolding of β**4** was characterized by CD at a number of cosolvent concentrations in the range 0−50% MeOH to determine the thermodynamic signature for folding and its solvent-dependence. In all cases, the thermal unfolding curves are incomplete in the temperature range accessible (283−353 K), demonstrating that these weakly folded systems, that lack the high degree of cooperativity evident for small proteins, undergo broad melting transitions. The temperature-dependence of the ellipticity was monitored at 217 nm (Figure 8a). In water alone, a very shallow melting profile was apparent, with evidence of cold denaturation below 310 K. Cold denaturation is still apparent in 10% MeOH but is not evident in 30% and 50% MeOH. The slope of the unfolding curve increases with increasing MeOH with evidence that θ_{217} reaches a limiting value of $-11\,600$ deg cm^2 mol^{-1} in 50% MeOH at low

Table 3. Thermodynamic Data for the Folding of β**4** from CD Melting Studies in Aqueous Methanol Solutions (0−50% v/v, pH 5.5, [peptide] = 50 μM)

solvent	ΔH (kJ mol^{-1})	ΔS (J K^{-1} mol^{-1})	ΔC_p (J K^{-1} mol^{-1})
aqueous solution	+11.9(±1.0)	+38(±3)	−465(±50)
10% (v/v) MeOH	+2.1(±1.5)	+11(±5)	−531(±73)
30% (v/v) MeOH	−17.8(±0.9)	−49(±3)	0[a]
50% (v/v) MeOH	−39.8(±3.0)	−106(±9)	0[a]

[a] Data fitted assuming $\Delta C_p \approx 0$; uncertainties in all parameters reflect fitting errors.

temperature. The calculated ellipticity for a fully folded β-sheet is close to this value.[37] Thus, we have taken this value as $\theta_{217}^{\text{limit}}$ for the fully folded state. The ellipticity for the fully unfolded peptide was estimated to be -600 deg cm^2 mol^{-1} from a peptide with an identical residue composition but a scrambled sequence, which shows no evidence from CD or NMR for folding in solution. Using eq 2, we have fitted the melting curves to determine ΔH, ΔS, and ΔC_p for folding at 298 K in the various solvent mixtures (Table 3). Previous studies have suggested that the hydrophobic effect diminishes significantly above 30% MeOH with $\Delta C_p \rightarrow 0$.[38] Consequently, $\Delta C_p = 0$ was used to fit the melting curves for 30% and 50% MeOH (Figure 8a). The calculated ΔH values for folding are shown in Figure 8b, establishing a linear relationship with [MeOH]. The data show that folding is enthalpically unfavorable in water alone ($\Delta H = +11$ kJ mol^{-1}), which, together with a positive ΔC_p, explains the observation of cold-denaturation and fits with a classical hydrophobic driving force.[39] However, folding becomes strongly enthalpy-driven as the concentration of the cosolvent increases, as is evident from protein folding studies in mixed solvents where the hydrophobic effect is largely negated.[38] The switch from an entropy-driven to enthalpy-driven mechanism appears to be consistent with the earlier conclusion that stabilization in water of a collapsed state is driven largely by hydrophobic contacts between side chains, but that cosolvents strengthen backbone hydrogen-bonding interactions as is evident from a switch to the enthalpy-driven folding mechanism.[7] The latter thermodynamic signature has been suggested to represent a tighter interaction that reflects a more cooperative folding process, stronger hydrogen bonds, and better van der Waals contacts, all of which contribute enthalpically to the stability of globular proteins but are largely masked by the thermodynamic signature of the hydrophobic effect. Proteins that fold in the presence of significant concentrations of cosolvents, where the hydrophobic contributions are significantly diminished, show similar enthalpy-driven folding parameters.[38] The nature of the stabilizing interactions also appears to play some part in modulating the balance between enthalpy and entropy contributions. Two hairpin systems containing an aromatic cluster of residues,[6g,8] and a three-stranded antiparallel β-sheet with a similar aromatic motif,[40]

(37) Greenfield, N.; Fasman, G. D. *Biochemistry* **1969**, *8*, 4108−4116.
(38) (a) Woolfson, D. N.; Cooper, A.; Harding, M. M.; Williams, D. H.; Evans, P. A. *J. Mol. Biol.* **1993**, *229*, 502−511. (b) Jourdan, M.; Searle, M. S. *Biochemistry* **2001**, *40*, 10317−10325.
(39) (a) Baldwin, R. L. *Proc. Natl Acad. Sci. U.S.A.* **1986**, *83*, 8069−8072. (b) Spolar, R. S.; Ha, J. H.; Record, M. T. *Proc. Natl. Acad. Sci. U.S.A.* **1989**, *86*, 8382−8385. (c) Dill, K. A. *Biochemistry* **1990**, *29*, 7133. (d) Blokzijl, W.; Engberts, J. B. F. N. *Angew. Chem., Int. Ed. Engl.* **1993**, *32*, 1545−1579.
(40) Griffiths-Jones, S. R.; Searle, M. S. *J. Am. Chem. Soc.* **2000**, *122*, 8350−8356.

all show enthalpy-driven folding in water without the effects of cosolvent additives.

Conclusions

We have used a model β-hairpin system of 16 residues to examine the energetic contribution to the stability of Glu−Lys salt bridges. We have mutated Ser residues at positions 6 and 15 to generate two salt bridges, one close to the β-turn (E_6−K_{11}), and one between residues close to the C- and N-termini (K_2−E_{15}). Individually, each interaction contributes ∼1.2−1.3 kJ mol^{-1} to stability, in agreement with previous studies;[17] however, when introduced simultaneously, the contribution (−3.6 kJ mol^{-1}) is greater than the sum of the individual contributions. Through a thermodynamic cycle, we suggest that the two interactions are cooperatively linked with the stabilizing effects of one interaction increasing the energetic contribution of the other through effects on the preorganization of the hairpin template.

Recent attempts to rationalize the extreme thermal tolerance of proteins from hyperthophilic organisms has focused on the optimization of electrostatic interactions by removing repulsive contacts and increasing the number of surface salt bridges.[15,16] Our data on a model hairpin system show that two Lys−Glu salt bridges, as replacements for two Lys−Ser pairs, cooperatively enhance the stability by −3.6 kJ mol^{-1}. The temperature-dependent behavior of this charge-stabilized folded conformation reveals a very broad melting transition in which the overall stability appears to be largely insensitive to temperature in the range 283−353 K. Thermodynamic analysis indicates entropy-driven folding with the enthalpy term unfavorable to folding at 298 K. In the presence of MeOH, the folded conformation becomes highly populated as folding becomes strongly enthalpy-driven.[7] The change in thermodynamic driving force with change in solvent composition appears to correlate with a change in the nature of the stabilizing interactions involved. The thermodynamic signature for folding in water indicates an entropy-driven mechanism consistent with a largely hydrophobically stabilized collapsed state with the stability modulated by electrostatic interactions from the introduced Glu−Lys pairs. The large change in the CD spectrum upon addition of cosolvents is consistent with the stabilization of a network of cross-strand hydrogen bonds that intensify the ellipticity at θ_{217} nm by ordering the peptide backbone.

Several recent molecular dynamics simulations have attempted to deconvolute the hydrophobic-driven collapse model from a more hydrogen bond centric zipper model of hairpin folding,[22] although others have suggested that the two are not mutually exclusive.[41,42] Many studies agree that hydrophobic residues make the largest contribution to stability and that cross-strand hydrogen bonding arises as a consequence of the strand alignment that is the inevitable consequence of optimizing hydrophobic contacts.[28] Simulations conclude that the turn region forms first, which is supported experimentally. In the current system, we have shown that a truncated peptide corresponding to residues 6−16 of β**1**, in which all hydrophobic residues along the N-terminal β-strand have been removed, shows good NMR evidence for formation of a type I′ turn centered around the SINGKK sequence.[4343] Following turn nucleation, hydrophobic collapse is considered to drive the interaction between β-strands with salt bridges helping to cement the hydrophobic core rather than drive folding because in polar solvents Coulombic interactions are relatively short range. Main chain amide hydrogen bonds between strands are proposed to form in the final step. In many simulations, hydrogen bonding between strands is weak;[42] whether their contribution to hairpin stability is correlated with hydrophobic surface area burial is unclear. In small peptide systems where relatively few weakly cooperative interactions are formed, and hydrophobic surface area burial is only modest, cross-strand hydrogen bonds are probably highly dynamic and energetically weak interactions. As is evident from the experimental studies described in this work, small peptide based systems that fold weakly in aqueous solution ($\Delta G \approx 0$) continue to provide insights into the energetics of weak interactions, their cooperative interplay, and the nature of the noncovalent forces that stabilize a variety of biomolecular assemblies.

Acknowledgment. M.J. acknowledges the European Community for a Marie-Curie research Fellowship. B.C. is supported by the BBSRC of the U.K. We thank the EPSRC of the U.K. for funding NMR and CD facilities within the School of Chemistry.

JA030074L

(41) Zhou, R. H.; Berne, B. J.; Germain, R. *Proc. Natl. Acad. Sci. U.S.A.* **2001**, *98*, 14931−14936.
(42) Tsai, J.; Levitt, M. *Biophys. Chem.* **2002**, *101*, 187−201.
(43) Griffiths-Jones, S. R.; Maynard, A. J.; Sharman, G. J.; Searle, M. S. *Chem. Commun.* **1998**, 789−790.